Preliminary investigation of elongation in RC walls

E. Encina & R. Henry

Department of Civil and Environmental Engineering, University of Auckland, Auckland

2015 NZSEE
Conference

ABSTRACT: Plastic hinge elongation in reinforced concrete (RC) structures has been observed in previous tests of components and subassemblies subjected to cyclic displacements. This elongation is caused by both geometric effects and residual crack widths, and has been shown to have a significant impact on the seismic behaviour of RC framed structures. Despite extensive research into the effects of member elongation on framed structures, few studies have investigated the influence of elongation in RC walls. A series of existing experimental tests were analysed to calculate RC wall axial elongation when subjected to cyclic loading and nonlinear fibre-type numerical models were developed to analyse their ability to accurately represent the axial elongation of RC walls. The experimental results confirmed that elongation is highly dependent on the axial load applied and the reinforcement distribution within the cross section. The proposed fibre-element model was able to simulate the elongations measured during the experimental tests with good accuracy.

1 INTRODUCTION

Ductile reinforced concrete (RC) walls in seismic regions are typically detailed considering capacity design methodologies to from plastic hinges at the wall base during severe earthquakes. The inelastic strains and cracking in the plastic hinge region results in an extension, or axial elongation, at the centre line of the wall. Plastic hinge elongation in RC frames has been extensively studied over the last 30 years. As described in Fenwick and Megget (1993), the mechanics of elongation in RC plastic hinges can be explained by geometric effects (temporary elongation) and residual crack widths (permanent elongation). Although the mechanics of elongation are fairly well understood by researchers and prediction of RC member elongation has been proposed in the literature, systematic analysis of RC wall elongation has not been conducted.

The elongation of RC walls will be partially restrained by other structural elements within a building, such as floors, beams and columns. As a result of this interaction, the RC wall elongation will alter both the loads generated in the wall and the loads generated in other structural elements. Chesi and Schnobrich (1987) described that due to elongation in the plastic hinge, the wall was subjected to increased compressive forces that led to an increase in shear demand and flexural strength. Additionally, studies by Wight (1985), Waugh and Sritharan (2010) and Henry et al. (2012) have highlighted the importance of considering wall-to-floor interaction due to the resulting additional flexural overstrength and an increased in wall axial load and shear demand. Consequently, it is important to account for RC wall elongation and wall-to-floor interaction when analysing and modelling the seismic behaviour of buildings with RC walls.

As part of an investigation of the seismic analysis of buildings accounting for wall-to-floor interaction, the elongation measured during seven previously conducted rectangular RC walls tests was calculated and analysed. In addition, nonlinear fibre-element models were constructed to assess the ability of this commonly used modelling technique to predict wall elongation.

2 ELONGATION IN RC MEMBERS

Geometric elongation and residual crack widths are primarily responsible for elongation of ductile RC hinges. While the former is a recoverable extension the latter is permanent. Geometric elongation arises when moment is applied to a cracked RC section, as can be seen in Figure 1a. Because the tensile strains in a cracked RC section are greater than the compressive strains there is a tension strain at the centre of the section, resulting in a net elongation. When inelastic cyclic displacements are imposed on an RC section, as shown in Figure 1b, yielding of longitudinal reinforcement and cracks in the concrete matrix trigger permanent elongation to arise. The permanent portion of the elongation is attributed to residual cracks caused by dislodged debris that prevents the cracks from fully closing. In addition, shear is transmitted through the wall by inclined compression struts, as presented in Figure 1c. To satisfy equilibrium the flexural tension force must be equal to the flexural compression forces plus the vertical component of the inclined compression strut. This mechanism results in less reinforcement stress in the compressive zone than those produced in the tensile zone and so the tensile strain cannot be fully recovered when load is reversed, thus accumulates during repeated reverse cyclic loading.

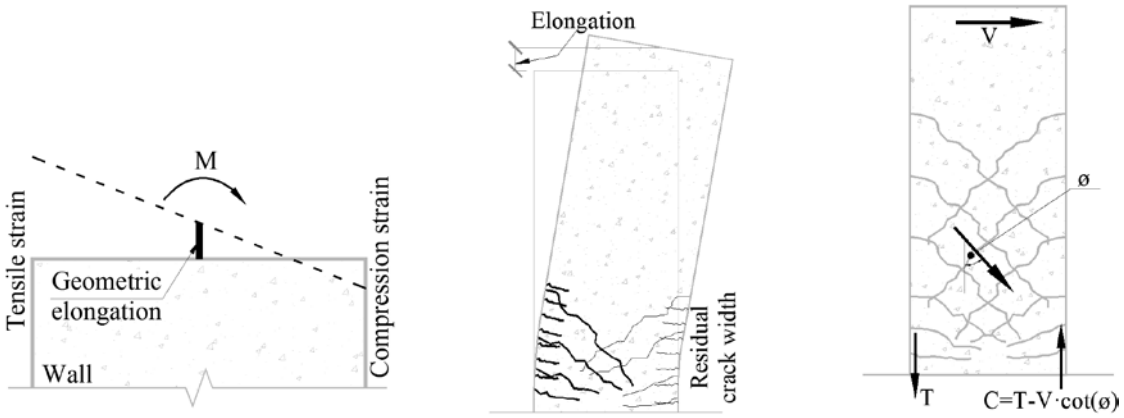

(a) Geometric elongation (b) Residual crack widths (c) Truss-like action

Figure 1. Elongation in RC walls.

In Figure 2a by Fenwick and Fong (1979), the flexural strain profiles measured during a RC beam test were plotted for 2 reverse cycles at displacement ductility demands of 2 and 4 (2D and 4D). After cycle +i the tensile strains at the bottom edge are not fully recovered when the loading is reversed and the bottom edge is placed in compression, leading to the permanent elongation of the beam. Figure 2b by Peng et al. (2007) presents the total elongation measured during the cyclic test of a cantilever beam. The elongation is observed to progressively accumulate throughout the test, with large residual elongations when the load is removed.

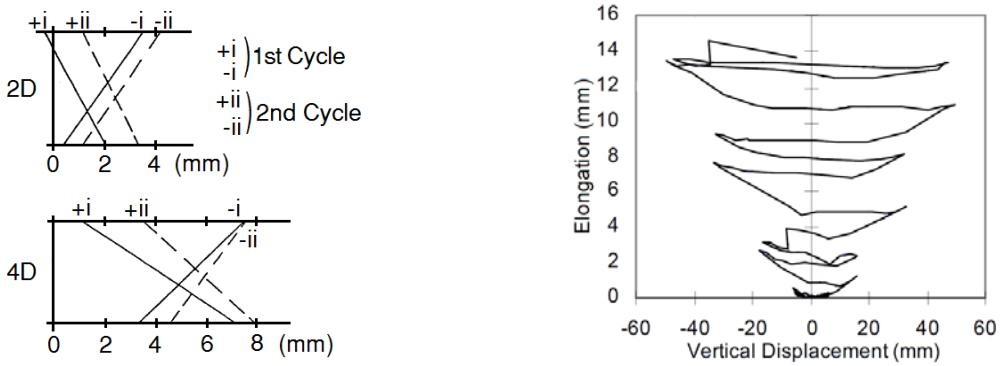

(a) Cyclic flexural strains Fenwick and Fong (1979) (b) Cyclic elongation Peng et al. (2007)

Figure 2. Examples of elongation measured during previous RC beam tests.

3 EXISTING EXPERIMENTAL DATA

Archived experimental data from four rectangular RC walls (PW1, PW2, PW3 and PW4) described in Birely (2012) and three rectangular RC walls (RWN, RWC and RWS) described in (Johnson 2007) and Aaleti et al. (2013) were used to investigate RC wall elongation when subjected to cyclic loading. General information about the test walls required to undertake the analysis and modelling is provided here; more detailed information is available in the aforementioned literature.

3.1 Walls PW1 to PW4

Walls PW1 to PW4 were part of the test program described by Lowes et al. (2011). The test walls represented the lower 3 levels of a one-third scale 10-storey RC wall, and were subjected to cyclic lateral displacements. Boundary conditions were applied at the top of the wall specimen to represent the loading of a 10-storey wall with axial load ratios of 9.6%, 13%, 10% and 11.7% applied during test PW1 to PW4 respectively. Cross sections of each test wall are shown in Figure 4. All test walls were 152 mm thick, 3048 mm long and 3658 mm tall. Walls PW1, PW2 and PW4 had lumped longitudinal reinforcement in the boundary region at the ends of the wall section and minimum reinforcement in the middle web region of the wall, while PW3 had uniformly distributed longitudinal reinforcement throughout the cross section. The boundary elements of walls PW1, PW2 and PW4 had a longitudinal reinforcement of 7 layers of 3×12.7 mm diameter reinforcement, which was confined by 6.35 mm diameter stirrups and cross ties spaced at 51 mm on centres. Longitudinal and transverse reinforcement in the web were composed by 2 layers of 6.35 mm diameter reinforcement spaced 152 mm on centres. Specimen PW3 had a longitudinal reinforcement in the boundary zones of 14 × 12.7 mm diameter reinforcement confined by 6.35 mm diameter stirrups and cross ties at 44 mm on centres. Longitudinal reinforcement in the wall web consisted of 12.7 mm diameter reinforcement spaced at 108 mm on centres, while transverse reinforcement was 6.35 mm diameter reinforcement spaced at 152 mm on centres.

(a) Cross section for PW1, PW2 and PW4

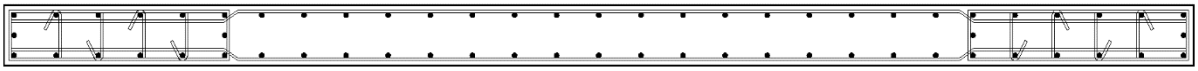

(b) Cross section for PW3

Figure 3. Schematic representation of wall cross sections of specimens PW1 to PW4.

3.2 Walls RWN, RWC and RWS

Walls RWN, RWC and RWS were part of a test program that investigated the behaviour of both rectangular and T-shaped walls. A total of three rectangular half-scaled 4-storey RC walls were tested with asymmetric reinforcement and no axial load. Cross sections of the specimens are provided in Figure 4. All three walls were 152 mm thick, 2286 mm long and 6400 mm tall and were subjected to an asymmetrical reversed cyclic lateral displacement. The three walls had the same arrangement of reinforcement, except that three different splices were investigated for the longitudinal reinforcement at the wall base, namely no splice, couplers and lap splice. Longitudinal reinforcement in the left boundary zone in Figure 4, hereafter referred to as #5#6BE, consisted of 4×19 mm diameter and 2 × 16 mm diameter reinforcement. Confinement of #5#6BE was provided by 6.35 mm diameter stirrups and cross ties spaced at 64 mm on centre. Reinforcement in the right boundary zone in Figure 4, hereafter referred to as #9BE, consisted in 8×28.7 mm diameter longitudinal bars, 4 of which were confined by 6.35 mm diameter stirrups spaced at 51 mm on centres. Vertical web reinforcement consisted in two layers of 12.7 mm diameter bars spaced at 458 mm on centres and horizontal reinforcement consisted in 2 layers of 9.5 mm diameter bars spaced at 190 mm on centres.

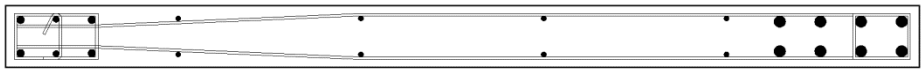

Figure 4. Schematic representation of wall cross section of specimens RWN, RWC and RWS.

3.3 **Experimental RC wall elongations**

The results of the calculated cyclic elongations for the seven RC wall tests are presented and analysed in this section. Special attention was given to the effect of axial load, reinforcement distribution, elongation at peak cyclic displacements, and residual elongations. The two latter parameters are defined as the elongation calculated in the wall when it reaches the maximum displacement of a particular cycle, and the elongation calculated in the wall when it returns to zero displacement after it was at a peak cyclic displacement, respectively.

Figure 5a presents the elongation history for PW1 that was subjected to an axial load of 9.6% of $A_g f'_c$, while Figure 5b shows the elongation history for RWN that was subjected to no axial load during the test. As can be observed elongation developed from the beginning of the tests and increased with drift. The overall elongation patterns of the RC walls were similar with those described in previous studies on beams, as shown in Figure 2b, but the accumulation of permanent elongations was less. A comparison of Figure 2b with Figure 5 highlights the potential influence of reinforcement distribution and axial load in the way elongation is produced in RC members.

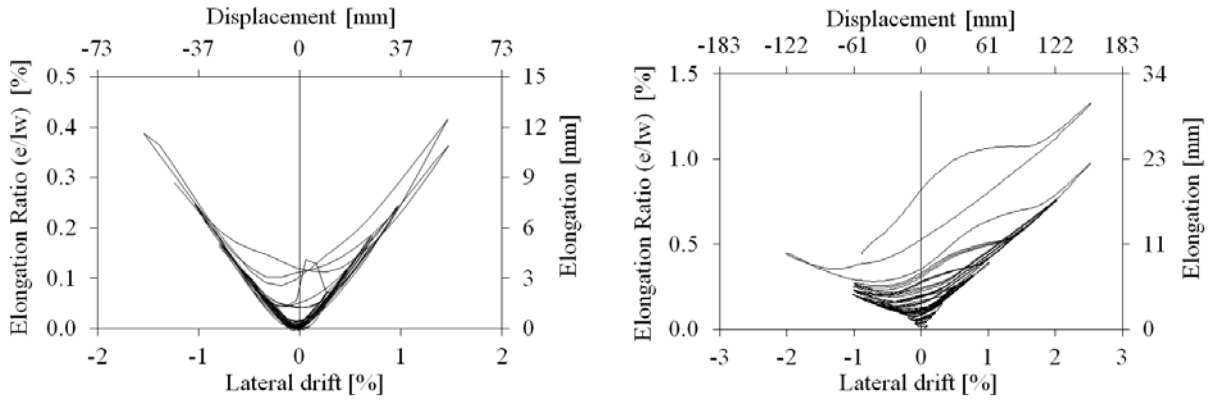

(a) History of cyclic elongation of wall PW1

(b) History of cyclic elongation of wall RWN

Figure 5. Measured cyclic elongations from RC wall tests.

When symmetrical reinforcement is placed at a section, as in the PW walls, elongation occurs symmetrically, with similar elongation magnitude irrespective of the direction of displacement. However, when an asymmetrical reinforcement layout is used in the wall greater elongations occur when the wall is subject to tensile stress in the boundary element with less reinforcement due to the smaller neutral axis depth, as highlighted by the larger elongation in the positive drift direction of wall RWN in Figure 5b. Axial load also had a noticeable influence on the measured wall elongation. Axial loads tend to reduce the accumulation of permanent elongation, with the wall response dominated by recoverable geometric elongation, as seen for wall PW1 in Figure 5a. Permanent elongations are more noticeable in wall RWN with no axial load. Considering the positive drifts of both PW1 and RWN in Figure 5, elongation ratio (e/lw) in RWN is almost twice of that in PW1 for 1.5% drift. It is also noteworthy the behaviour of the residual elongation for RWN and PW1, where the difference between them can reach up to 4 times.

The elongation parameters calculated from the seven RC wall tests are presented in Figure 6. The elongations at peak cyclic displacement are shown in Figure 6 (a) and (c), and the residual elongations at zero drift are shown in Figure 6 (b) and (d). In the case of the PW-walls, the presence of axial load minimised the initial tendency of the walls to elongate up to a drift of about 0.35%. The behaviour of the elongation beyond drift of 0.35% follows a linear trend, but the slope is affected by axial load with

slightly larger elongation occurring for PW1. By comparing the residual elongations from the PW and RW walls, it is clear that an axial load of 10% of $A_g f'_c$ or greater will reduce the residual elongation to almost zero. By contrast, the RW-walls were not subjected to axial loads and greater residual elongation occurred, ranging between 0.4% and 0.6% of the length of the wall.

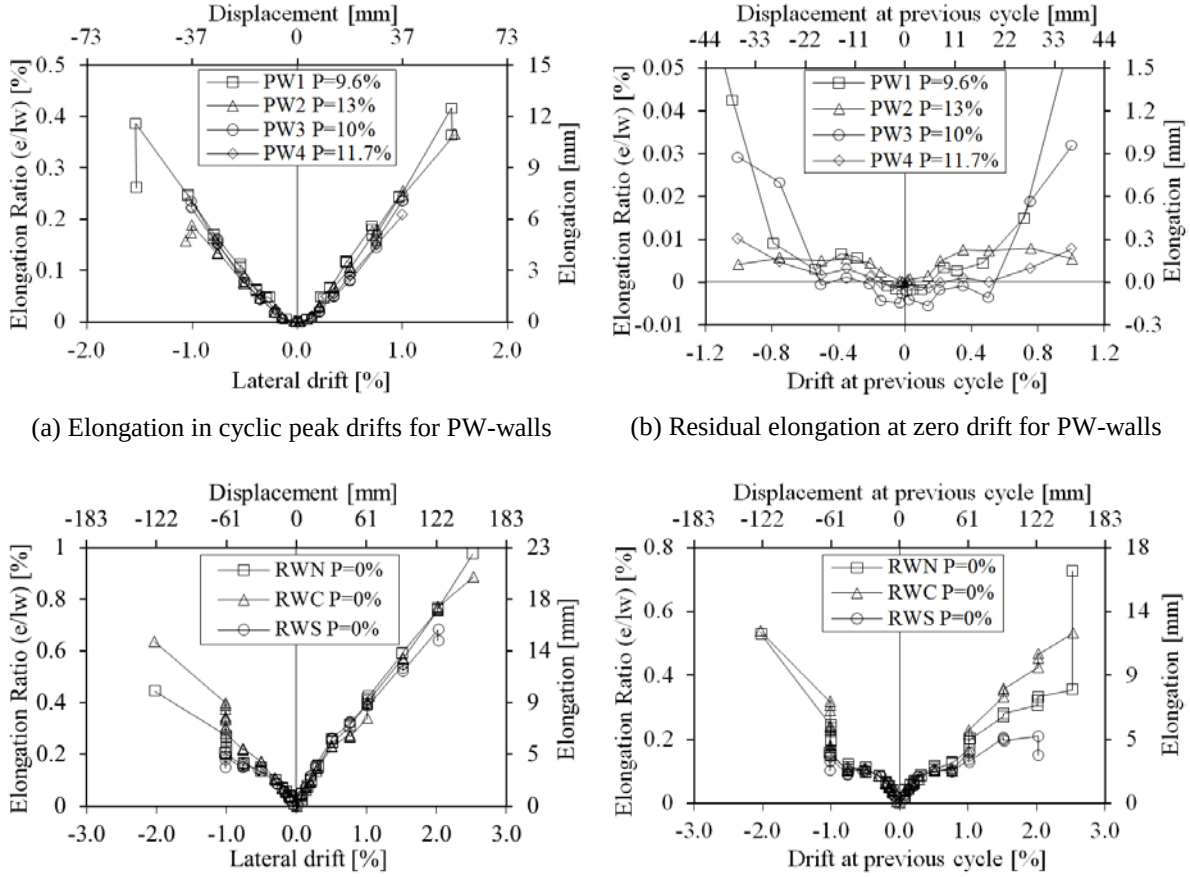

(a) Elongation in cyclic peak drifts for PW-walls

(b) Residual elongation at zero drift for PW-walls

(c) Elongation in cyclic peak drifts for RW-walls

(d) Residual elongation at zero drift for RW-walls

Figure 6. Elongation parameters for PW-wall and RW-wall tests.

When symmetric cycles at the same drift were applied, the change in elongation on subsequent drift cycles to the same displacements was negligible. It is worth noting that in the case of RW walls nine cycles to 1% drift were applied with the #5#6BE boundary element in tension, while drift cycles with the #9BE boundary element in tension increased from 1%, to 1.5%, to 2% drift. This asymmetric loading resulted in significant increase in both peak and residual elongations at -1% drift for RW walls.

4 NUMERICAL MODEL

4.1 Model description

The aim of the numerical model was to develop an efficient method to represent the cyclic behaviour of RC walls that could be easily implemented in a model of an entire building. Many of the models proposed in the literature capture the elongation by representing the cross section with discretise nonlinear fibre-type elements (Fenwick and Davidson 1995, Lee and Watanabe 2003, Peng et al. 2007, Eom and Park 2010, Eom et al. 2013). Fibre-type beam-column elements have been extensively used to represent the flexural behaviour of RC walls and so a distributed-plasticity fibre-based beam-column element, as described by Spacone, et al. (1996), were selected to model the walls for this investigation. According to Neuenhofer and Filippou (1997), force-based fibre elements provide a

better representation of inelastic region of RC elements. Additionally, Martinelli and Filippou (2009) suggest that when using force-based elements and there are no external loads within the element but the nodes, three to four integration points provide sufficient accuracy to represent the plastic hinge regions.

Force-based element formulation assumes linear moment and constant axial force within the element, so the model meshing was provided accordingly. The RC wall model used to represent the RW and PW tests described in section 3 is presented in Figure 7. The model was implemented in OpenSees (McKenna, Scott and Fenves 2006) using a distributed-plasticity fibre-based beam column element with force formulation to represent axial force bending interaction and an aggregate linear elastic material to represent shear deformation. Oyen (2006) developed a nonlinear technique to simulate wall response to lateral loads when modelled with distributed-plasticity beam-column elements and recommended the use of a modified shear modulus to account for shear displacement and bar slip.

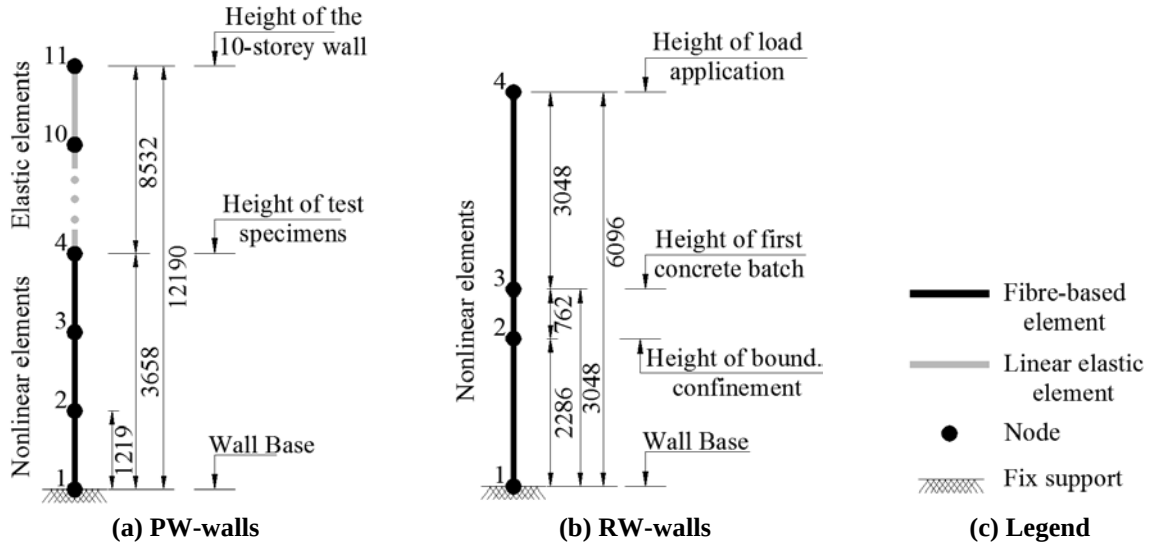

(a) PW-walls **(b) RW-walls** **(c) Legend**

Figure 7. Schematic representation of numerical models.

Uniaxial constitutive material models were used to describe the nonlinear material behaviour of the fibres within the element, and P-Delta formulation was used to represent the nonlinear geometric behaviour. Concrete material utilised was the modified Kent-Park model with linear tension softening, as described in (Yassin 1994) and available in OpenSees as Concrete02. Compressive behaviour of Concrete02 has an ascending parabolic branch and a linear descending branch until a residual compressive strength. The tensile behaviour is defined by a bi-linear curve with zero residual strength.

The reinforcing steel was simulated using the Menegotto and Pinto (1973) nonlinear model, modified by Filippou, Popov and Vertero (1983) to include isotropic strain hardening and available in OpenSees as Steel02. The stress-strain relationship of Steel02 is described by a linear elastic curve with slope E_0 (steel's elastic modulus) and then, when close to yielding, curves and follows an asymptote with slope $b \cdot E_0$ (strain hardening slope; $b<1$). Unload and reload path capture the Bauschinger effects. A graphical representation of both the concrete and steel materials models is shown in Figure 8.

Unconfined concrete properties and reinforcing steel properties were based on the material tests data available in Birely (2012) and Johnson (2007), and the confined concrete properties were calculated according to the model proposed by Mander et al. (1988). When material properties were not available, nominal values were assumed and model properties were obtained, when needed, from Collins and Mitchell (1997) for unconfined concrete in compression and from the fib 2010 Model code (fib Bulletin 65 2012) for tensile concrete behaviour. Materials were assigned to the corresponding fibres according to their actual position in the wall cross-section.

Fibre discretization was selected by iteration taking on account solution convergence of the model and invariability of results. For walls PW1, PW2 and PW4 20 layers for the boundary zones and 60 layers for the web zone were used. Wall PW3 used 25 layers for the boundary zones and 55 layers for the web. In the case of walls RWC, RWN and RWS 40 layers were needed in the #5#6BE, 30 layers in the #9BE and 100 layers in the web zone.

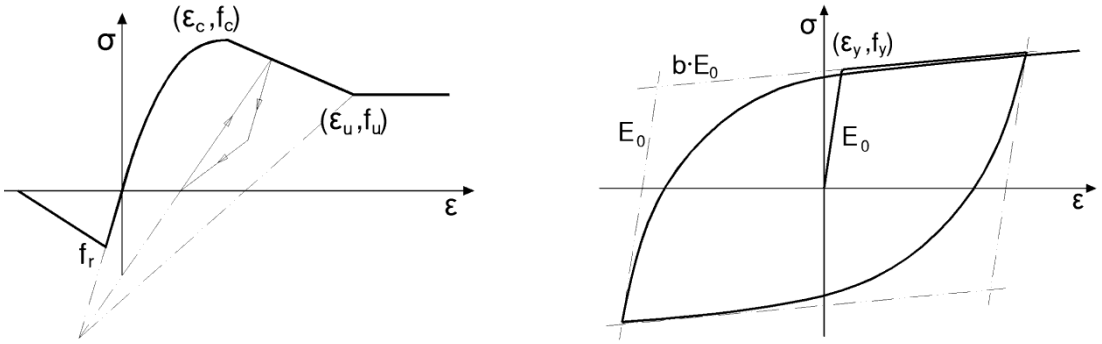

(a) Schematic concrete stress-strain curve **(b) Schematic reinforcing steel stress-strain curve**

Figure 8. Constitutive material models.

The RC walls were tested with reverse cyclic loading and so the simulation was conducted using a sequence of concatenated pushover analyses. The first analysis step applied the gravity loads to the models and then the cyclic pushover was conducted by pushing the walls to a series of lateral displacement as per the loading protocol applied during the experimental tests.

4.2 **Model validation**

Validation of the numerical model was performed by comparison of the results for both experimental and simulated elongations. In order to check the ability of the models to represent the global response of the wall specimens force-displacement and moment-displacement curves were compared for all seven wall tests. As a representative sample, the simulated and experimental force-displacement charts for PW1 and RWN are presented in Figure 9. It can be observed that the simulated behaviour from the fibre model matches the experimental responses with good accuracy. In general, the completeness of data for the PW-walls allowed for a more accurate simulated response than the RW-walls. Despite this fact, the RW wall hysteresis response was still captured with sufficient accuracy by the numerical models.

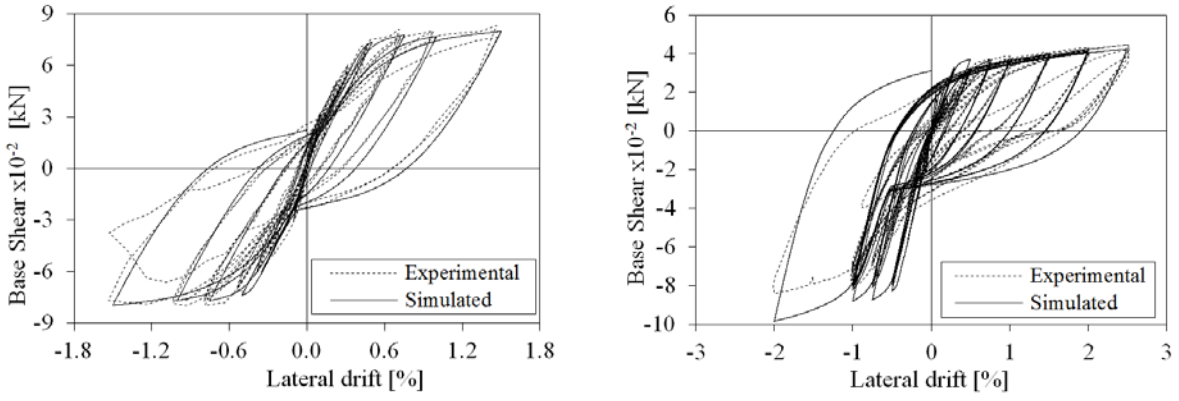

(a) PW1 (b) RWN

Figure 9. Representative lateral force-displacement behaviour for PW-walls and RW-walls.

The capabilities of the model to represent wall elongation was analysed by comparing the simulated elongation with the measured elongations presented in section 3.3 for the peak envelope and residual elongation data. The comparisons of the elongation parameters for PW-walls are shown in Figure 10 while the comparisons of elongation parameters for RW-walls are shown in Figure 11. In the case of the PW-walls, good agreement between simulated and experimental elongation data can be observed. Initial elongation at peak displacements was well modelled up to 0.35% drift, over which drift the models tended to overpredict elongation by up to 20% on average at the end of the test. Predicted residual elongations were in overall agreement with those previously calculated from the experimental tests. For PW-walls the residual elongation were extremely small, ranging between -0.15 to 0.3 mm as can be observed in Figure 6b, and as a result were difficult to predict precisely.

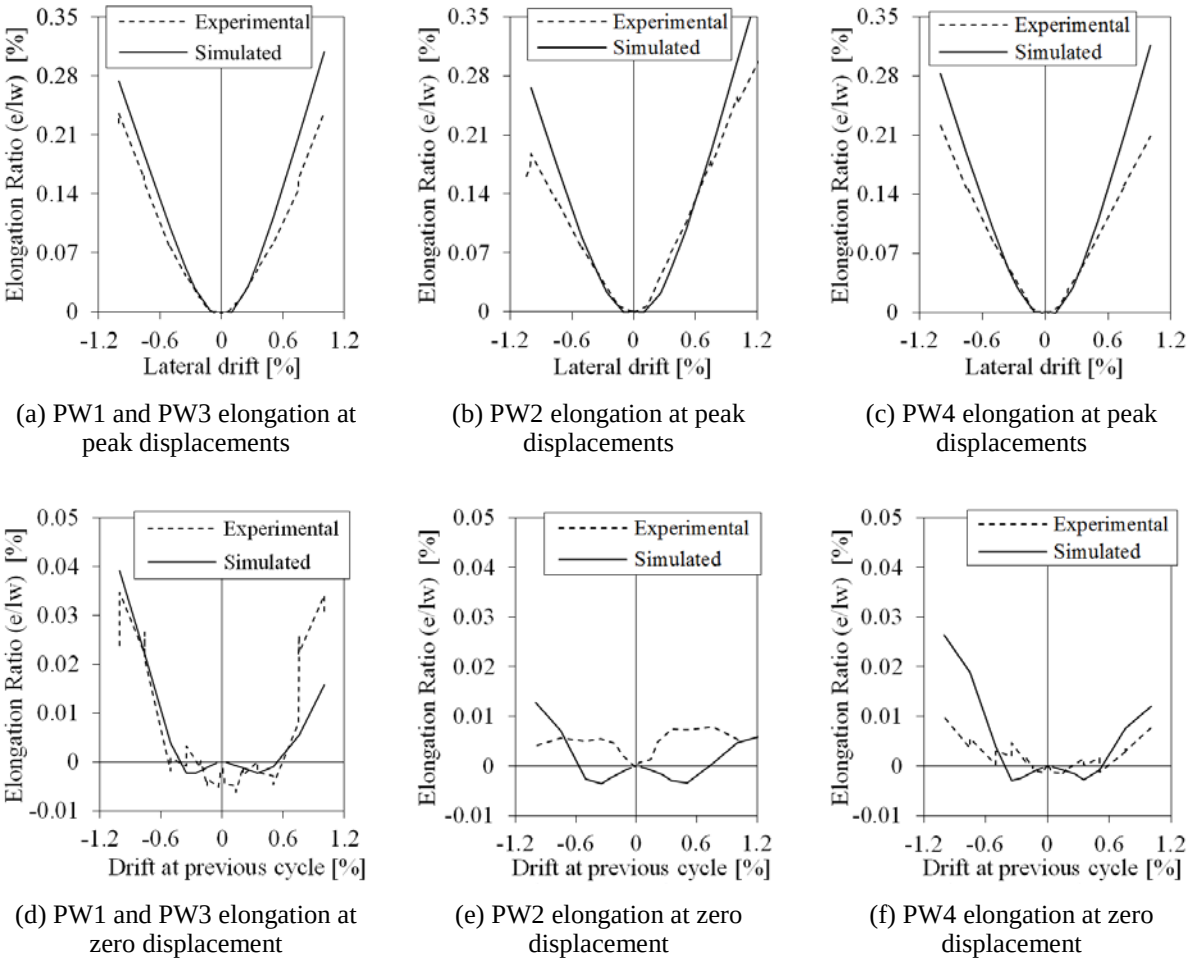

(a) PW1 and PW3 elongation at peak displacements

(b) PW2 elongation at peak displacements

(c) PW4 elongation at peak displacements

(d) PW1 and PW3 elongation at zero displacement

(e) PW2 elongation at zero displacement

(f) PW4 elongation at zero displacement

Figure 10. Comparison of predicted elongation for PW-walls.

As shown in Figure 11, the predicted elongation for RWN and RWC walls was also in good agreement with the experimental data within the test displacements for peak elongations and up to 1.0% drift for residual elongations. The elongations beyond these drifts were overestimated by the model, specially the case when walls were pushed to negative displacement over 1.0% drift, after which overestimations of about 25% were made at the end of the tests. The residual elongations of walls RWN and RWC were well estimated by the model, following similar paths between -1.0% and 2.0% drift, after which the residual elongation tends to stop growing when returning from positive drifts and tend to grow faster when returning from negative drifts. For the RWS wall, the model was not able to capture the residual elongation, whereas the peak elongation was well capture. This difference between the simulated and experimental residual elongations for RWS are likely due to the fractured of the #5#6BE boundary element during the test which led to the premature weakening of the section.

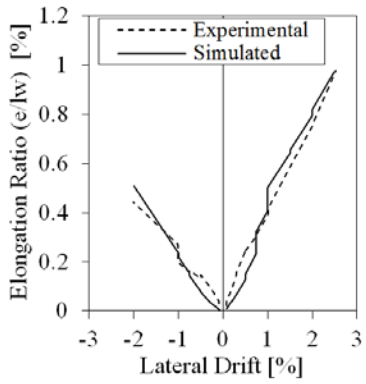

(a) RWN and RWC elongation at peak displacements

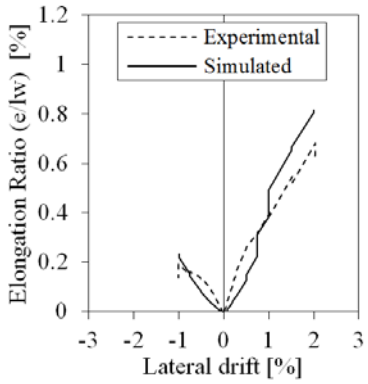

(b) RWS elongation at peak displacements

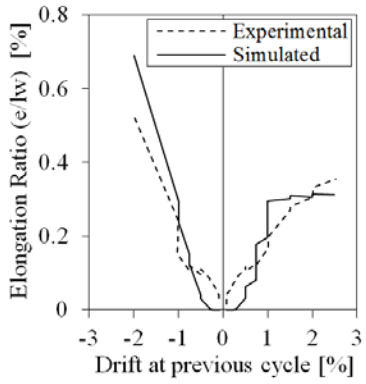

(c) RWN and RWC elongation at zero displacements

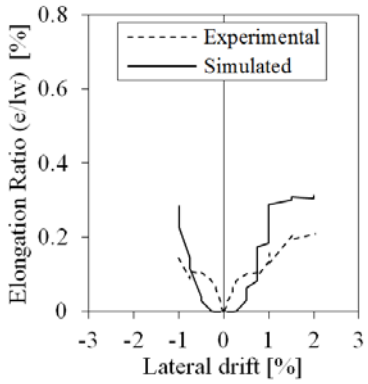

(d) RWS elongation at zero displacements

Figure 11. Comparison of predicted elongation for RW-walls.

5 CONCLUSIONS

Axial elongation of rectangular RC walls was investigated based on experimental data from seven previously conducted RC wall tests. The experimental results were used to validate a numerical model developed in OpenSees to simulate elongation of RC walls. The model utilised distributed-plasticity fibre-based beam-column elements with force formulation to represent the walls. Based on this analysis the following conclusions were made:

- Axial compression load tends to decrease the accumulation of permanent elongation, with the response dominated by recoverable geometric elongation.
- The proposed numerical model captured elongation well up to an average of 1.0% drift for both elongation at peak and zero displacement.
- The average elongation ratio (elongation as percentage of wall length) at peak displacements for both PW and RW walls were 0.21% and 0.6% respectively.
- Average residual elongation ratios for PW and RW walls were 0% and 0.35% respectively.

Future development of this research will include: 1) addition of new experimental data, 2) development of an improved model able to accurately capture elongation at higher drifts, 3) conducting building analysis considering elongation and wall-to-floor interaction.

6 ACKNOWLEDGEMENTS

The authors wish to acknowledge the Chilean Government for awarding the first author with a Becas Chile scholarship for his doctoral study at the University of Auckland. Financial support for this research was provided by the Natural Hazards Research Platform through contract C05X0907. The experimental data used during this investigation was downloaded from the NEES Hub data repository, listed as project number NEES-2005-0022 and NEES-2005-0104.

7 REFERENCES

Aaleti, S., Brueggen, B.L., Johnson, B., French, C. & Sritharan, S. 2013. Cyclic Response of Reinforced Concrete Walls with Different Anchorage Details: Experimental Investigation. *Journal of Structural Engineering*, 139: 1181-1191.

Birely, A. 2012. Seismic Performance of Slender Reinforced Concrete Structural Walls. Ph.D. Thesis, University of Washington, Washington, USA.

Chesi, C. & Schnobrich, W.C. 1987. 3-Dimensional Contribution to frame-wall Lateral Behavior, in *Civil Engineering Studies, S.R.S.N. 531*, Editor. 1987, University of Illinois at Urbana-Champaign.

Collins, M.P. & Mitchell, D. 1997. *Prestressed Concrete Structures*, Toronto, Ontario.

Eom, T. & Park, H. 2010. Elongation of Reinforced Concrete Members Subjected to Cyclic Loading. *Journal of Structural Engineering*, 136(9): 1044-1054.

Eom, T., Park, H., Kim, J., & Lee, H. 2013. Web crushing and deformation capacity of low-rise walls subjected to cyclic loading. S*tructural Journal*, 110(4): 575-584.

Fenwick, R.C. & Davidson, B. J. 1995. Elongation in Ductile Seismic-Resistant Reinforced Concrete Frames. Thomas Paulay Symposium, Vol. 157.

Fenwick, R.C. & Fong, A. 1979. The Behaviour of Reinforced Concrete Beams under Cyclic Loading. *Bulletin of the NZSEE*. 12(3): 158-167.

Fenwick, R.C. & Megget, L.M. 1993. Elongation and Load Deflection Characteristics of Reinforced Concrete Members Containing Plastic Hinges. *Bulletin of the NZSEE*, 26(1): 28-41.

fib Bulletin 65 2012, Model code 2010. fédération internationale du béton *fib*), Lausanne, Switzerland.

Filippou, F.C., Popov, E.P. & Bertero, V.V. 1983. Effects of bond deterioration on hysteretic behavior of reinforced concrete joints. Technical Report EERC-83/19, Earthquake Engineering Research Center, University of California, Berkeley.

Henry, R.S., Ingham, J. & Sritharan, S. 2012. Wall-to-floor interaction in concrete buildings with rocking wall systems, NZSEE Conference, Christchurch, New Zealand.

Johnson, B.M. 2007. Longitudinal Reinforcement Anchorage Detailing Effects on RC structural Wall Behavior. M.Sc. Thesis, University of Minnesota, Minnesota, USA.

Lee, J. & Watanabe, F. 2003. Shear Deterioration of Reinforced Concrete Beams Subjected to Reversed Cyclic Loading. *ACI Structural Journal*, 100(4): 480-489.

Lowes, L.N., Lehman, D., Birely, A.C., Kuchma, D., Marley, K. & Hart, C. R. 2011. "Behavior, Analysis, and Design of Complex Wall Systems: Planar Wall Test Program Summary Document," https://nees.org/resources/3677.

Mander, J.B., Priestley, M.J.N. & Park, R. 1988. Theoretical Stress-Strain Model for Confined Concrete. *Journal of Structural Engineering*, 114(8): 1804-1826.

Martinelli, P. & Filippou, F.C. 2009. Simulation of the Shaking Table Test of a Seven-story Shear Wall Building. *Earthquake Engineering and Structural Dynamics*, 38: 587-607.

McKenna, F., Scott, M.H. & Fenves, G.L. 2006. Open System for Earthquake Engineering Simulation, Pacific Earthquake Engineering Research Center, University of California, Berkeley.

Menegotto, M. & Pinto, P. 1973. Methods of analysis for cyclically loaded R/C frames. Proceedings of the Symposium of Resistance and Ultimate Deformability of Structure Acted by Well Defined Repeated Load, IABSE, Lisbon, Portugal.

Neuenhofer, A. & Filippou, F.C. 1997. Evaluation of nonlinear frame finite-element models. *Journal of Structural Engineering*, 123(7): 958-966.

Oyen, P.E. 2006. Evaluation of Analytical Tools for Determining the Seismic Response of Reinforced Concrete Shear Walls. M.Sc. Thesis, University of Washington, Washington, USA.

Peng, B.H.H., Dhakal, R.P., Fenwick, R.C., Carr, A.J. & Bull, D.K. 2007. *Analytical Model on Beam Elongation within the Reinforced Concrete Plastic Hinges*, NZSEE Conference, New Zealand.

Spacone, E., Filippou, F.C. & Taucer, F.F. 1996. Fibre Beam-Column Model for Non-Linear Analysis of R/C Frames: Part I. Formulation. *Earthquake Engineering and Structural Dynamics*, 25(7): 711-725.

Waugh, J.D. & Sritharan, S. 2010. Lessons Learned from Seismic Analysis of a Seven-Story Concrete Test Building. *Journal of Earthquake Engineering*, 14(3): 448-469.

Wight, J.K. Ed. 1985. Earthquake effects on reinforced concrete structures: U.S.-Japan Research. Detroit.

Yassin, M.H. 1994. Nonlinear Analysis of Prestressed Concrete Structures under Monotonic and Cyclic Loads. PhD. Thesis, University of California, Berkeley.